

RESEARCH

Open Access



Optimization of structural reinforcement assessment for architectural heritage digital twins based on LiDAR and multi-source remote sensing

Yanru Shi¹, Ming Guo^{1,2,3*}, Jiawei Zhao¹, Xuanshuo Liang¹, Xiaoke Shang¹, Ming Huang¹, Shuai Guo¹ and Youshan Zhao^{4*}

Abstract

This study investigates the geometric modelling of architectural heritage digital twins constructed based on multi-source point cloud data and its effectiveness in structural reinforcement assessment. Particular emphasis has been placed on the use of static stiffness rules to identify areas of structural weakness in the geometric models of digital twins and the need for their reinforcement, in order to prevent potential structural problems and to ensure the long-term preservation of the built heritage. Taking Yingxian wooden pagoda as a study case, based on the collection of multi-source point cloud data, the digital twin geometric model is constructed through fine modelling, decoupling of digital models, and geometric transformation. This enhances the true reflection of the column-architrave structure morphology, providing a more accurate model for structural stress analysis. Based on verifying the accuracy of the digital twin geometric model, the instability conditions are identified through static stiffness rules and the deformation values at multiple points are analyzed, enabling precise identification of weak areas in the column-architrave structure. Two types of reinforcement measures are designed and simulated for the structural weak areas identified through the geometric modelling, and the optimal reinforcement scheme is obtained after detailed analysis, according to which specific adjustments and optimization strategies are proposed to enhance the overall stability and durability of the structure. The results showed that the maximum deformation value of 4.65 mm existed in column M2W23, which required reinforcement. Aluminum reinforcement reduced the deformation to 3.5 mm (24.7% reduction), while CFRP fabric reinforcement was more effective, reducing the deformation to 2.8 mm (39.7% reduction), showing high stability. The research results demonstrate the potential application of digital twin technology in architectural heritage preservation and restoration, providing methodological and empirical guidance for heritage preservation research.

Keywords Architectural heritage structure, Digital twin geometric model, Reinforcement effects, Numerical simulation

*Correspondence:

Ming Guo
guoming@bucea.edu.cn
Youshan Zhao
yshzhao@163.com

Full list of author information is available at the end of the article



© The Author(s) 2024. **Open Access** This article is licensed under a Creative Commons Attribution 4.0 International License, which permits use, sharing, adaptation, distribution and reproduction in any medium or format, as long as you give appropriate credit to the original author(s) and the source, provide a link to the Creative Commons licence, and indicate if changes were made. The images or other third party material in this article are included in the article's Creative Commons licence, unless indicated otherwise in a credit line to the material. If material is not included in the article's Creative Commons licence and your intended use is not permitted by statutory regulation or exceeds the permitted use, you will need to obtain permission directly from the copyright holder. To view a copy of this licence, visit <http://creativecommons.org/licenses/by/4.0/>. The Creative Commons Public Domain Dedication waiver (<http://creativecommons.org/publicdomain/zero/1.0/>) applies to the data made available in this article, unless otherwise stated in a credit line to the data.

Introduction

Architectural heritage, as a core aspect of Chinese culture, holds significant historical and social value. However, after nearly a millennium, these structures often face issues like component aging, biological erosion, and human damage, leaving many in a deteriorated condition. Deterioration in the performance of architectural heritage structures leads to premature structural deterioration or collapse, and any lack of precision and scientific reinforcement often results in irreversible damage. Therefore, architectural heritage structures need to be scientifically and accurately reinforced and maintained to ensure their stability and durability. Especially for ancient wooden structures, their fragility and irreversibility make it necessary to take accurate and efficient wooden structure reinforcement and protection measures, otherwise the reinforcement and protection effect of various types and degrees of wooden structure damage will not be guaranteed, which will lead to immeasurable cultural heritage loss and social impact. Digital twin technology has the capability to maintain structural integrity and perform optimization adjustments. Digital twin technology for architectural heritage can timely identify potential weak areas in structures and provide scientific and precise restoration decision-making support. Therefore, there is an urgent need to develop interdisciplinary collaboration in the optimization of structural reinforcement assessment for architectural heritage digital twins based on LiDAR and multi-source remote sensing. Using the digital twin geometric model of architectural heritage, the mechanical properties and structural behavior of the structural geometric model are studied in depth. Based on the static stiffness rules to identify the weak areas of the structure, targeted design and analysis of reinforcement measures, and digital twin adjustment and optimization strategies. This research contributes to extending the service life of architectural heritage and preserving its precious cultural heritage value.

Scholars at home and abroad have conducted a number of studies on digital twinning, deformation monitoring, mechanical characterization and structural reinforcement of architectural heritage. There has been some discussion among scholars about the concept of digital twin technology, describing a variety of representations of digital twins in terms of digital copies, dynamic virtual representations, and other aspects [1–4]. Digital twins have been reported and in demand for applications in a variety of fields such as electric power [5], automotive [6], healthcare [7], urban geographic information [8], and road materials [9]. However, research on the application of digital twin technology in the field of architectural heritage is still in the primary stage of exploration, and many scholars are conducting preliminary exploratory

studies [10, 11]. Li et al. summarized relevant techniques involving architectural heritage preservation in terms of the disaster cycle and digital phases [12]. Tan et al. conducted a study on archaeological dating of architectural heritage using tools such as laser scanning and tilt photogrammetry in conjunction with digital twin technology [13]. Guo [14, 15] and others conducted an exploratory study on data support for architectural heritage digital twins through surveying and mapping techniques. The above studies have both demonstrated the potential of the technique for consolidation and preservation, while at the same time emphasizing that the applicability of the technique in diverse building types is still limited. In addition, systematic research on the effective use of the technique for the assessment and optimization of consolidation of architectural heritage is still in the early stages. LiDAR and 3D modelling technologies play a critical role in cultural heritage preservation through their high-precision measurements and wide spatial coverage capabilities. These technologies improve the efficiency and usefulness of data analysis by enabling rapid, non-contact data collection, effectively monitoring changes in the structure of ancient buildings and helping to verify the effectiveness of reinforcement measures. Specifically, Cabaleiro and Branco et al. combined borehole testing and laser scanning to calculate and apply residual cross sections to a 3D model [16, 17]. Some research scholars [18–20] used the wooden pagoda in Yingxian County as the research object to obtain the tilt and deformation condition of the single column, single layer and the whole of the wooden pagoda by using LiDAR technology. Some researchers explored the deformation characteristics of the arch nodes, vertical compression stiffness and vertical load transfer characteristics [21, 22]. Subsequently, Xue et al. [23, 24] further clarified the effects of compressive strength, modulus of elasticity and coefficient of friction of wood on its force performance by using arch footing specimens as the research object. In the study of the mechanical properties of nodes of column footing structures, He et al. [25, 26] focused on the footing nodes and analyzed the influence of rigid nodes on the force performance of the frame and the bending moment of the frame. Other researchers have specifically investigated the mechanical properties of column footings by modelling the specimens and performing static load tests [27–29]. However, there is still a lack of holistic studies for external columns and architraves of architectural heritage. In the context of structural strengthening assessment of architectural heritage structures, Xue et al. [30, 31] experimented with straight mortise and tenon joints by using different quantities of memory alloy wires and developed a novel friction damper to enhance the structure of mortise and tenon joints. A number of

scholars have investigated the mechanical behavior and reinforcement effect of specimens using novel materials to reinforce aged wood [32, 33]. By analyzing the bending moment-rotation relationship of through-tenon joints and verifying it with quasi-static tests, the researchers provided a mechanical model for the reinforcement of wood structures, and found that increasing the tenon size and the length of the self-tapping screws could effectively reinforce the wood specimens, thus improving their earthquake resistant performance [34, 35]. Although some progress has been made, research on the reinforcement of structurally weak areas in architectural heritage still needs to be further deepened.

The research on establishing digital twin geometric models based on point cloud data and conducting reinforcement optimization is relatively limited in the aforementioned content. Based on this, this paper takes the Yingxian wooden pagoda as the research object, and carries out research on the optimization of structural reinforcement assessment for architectural heritage digital twins based on LiDAR and multi-source remote sensing. The research roadmap is shown in Fig. 1 below. Multi-source high-precision point cloud data were acquired by using LiDAR, which was modelled by fine modelling→decoupling of digital models→geometric transformation in order to construct a digital twin geometric model; Numerically simulate the deformation

of the digital twin geometry model and compare it with the real-time monitored deformation data to validate the accuracy of the geometry model; Based on static stiffness rules and multi-point deformation values in order to obtain weak regions in the second layer column-architrave structure; The weak areas of the column-architrave structure were reinforced and simulated to analyze their effects, and according to the simulation results of the digital twin system, a comprehensive optimization strategy including real-time monitoring, scenario analysis and risk management was recommended.

Geometric modelling of digital twins by LiDAR

Digital twins and structures overview

Digital twins overview

In the twin space, a five-dimensional framework is used to construct a digital twin model of the ancient architectural physical entity, and this framework includes the historical building physical entity (HBPE), the historical building digital twin (HBDT), the historical building twin data (HBDD), the services provided by the digital twin (HBSs), and the connectivity relationship between different dimensions (HBCN). Where the historical building digital twin can be expressed in terms of four model dimensions: geometric (M_G), physical (M_P), behavioral (M_B) and rule (M_R). In particular, the geometric model covers the geometry, dimensions and

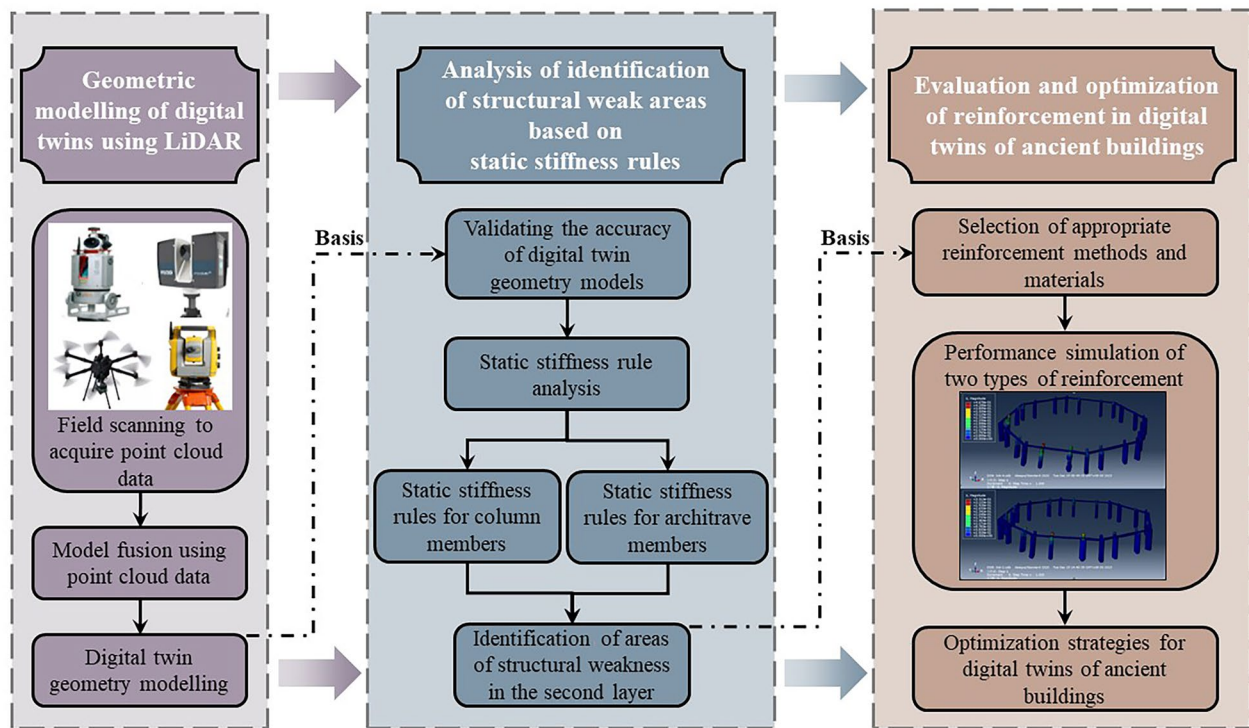


Fig. 1 Roadmap for research

assembly relationships between the components of the historical building entity, ensuring that the digital model is visually and structurally consistent with the physical historical building, and providing a model basis for subsequent analysis. Physical models reflect the physical properties of historic buildings, such as material properties and structural strength. Behavioral models represent the dynamic correspondence of historic buildings in response to internal and external mechanisms, and help to provide guidance for reinforcement. The rule model, built from extensive historical data and tacit knowledge of heritage buildings, enables the digital twin model to be highly intelligent and interact effectively in real-time with the physical structure, offering an advanced analytical tool for the preservation and maintenance of these buildings. This study focuses on finely describing the geometric model and applying static stiffness rules to identify potential weak regions in the structure. The organizational structure of the digital twin of the historical building is shown in Fig. 2.

Building structure overview

This study is based on a wooden pagoda located in Ying County, Shanxi Province. This pagoda possesses a complex structure of ten layers, including five obvious layers of the main pagoda body and five more hidden layers of the base and top. The total height of the tower is 67.31 m, consisting of a 4.4-m-high masonry base, a 51.14-m wooden main structure, a 1.86-m brick base and a 9.91-m iron spire at the top, from bottom to top. The base of the tower has a diameter of 30.27 m and is designed in

an octagonal plan. The study focused on the second layer of the tower’s structure, and by analyzing the point cloud data and deformation monitoring data accumulated over time, it was confirmed that the columns on the second layer were suffering from a more serious tilt problem. In particular, 24 peripheral columns (numbered from M2W1-S to M2W24-S) and eight architraves (numbered from F1 to F8) at the second layer were involved in the study to explore their structural integrity and maintenance requirements. The detailed size of the structure is shown in Fig. 3a and the front view of the structure is shown in Fig. 3b.

3D scanning and model data fusion programs

On-site 3D scanning and registration program

In order to obtain point cloud data for the Yingxian wooden pagoda, a combination of external and internal scanning methods was used, using Faro and Riegl scanners as well as UAV tilt photogrammetry. Applicable instruments include the Faro Focus3D X130 for close-range 3D laser scanning, covering a range of 50 m with millimeter-level target accuracy, and the DJI Phantom 4 RTK drone for low-altitude photogrammetry, with a centimeter-level positioning system and a highly efficient imaging system. The RIEGL VZ-4000 scanner enables distance measurement up to 4KM and supports multiple target echo recognition. During the acquisition of the external point cloud data, we first used a holistic registration method; for the internal point cloud data, we performed a preliminary registration by identifying features, followed by an iterative closest point (ICP) algorithm for

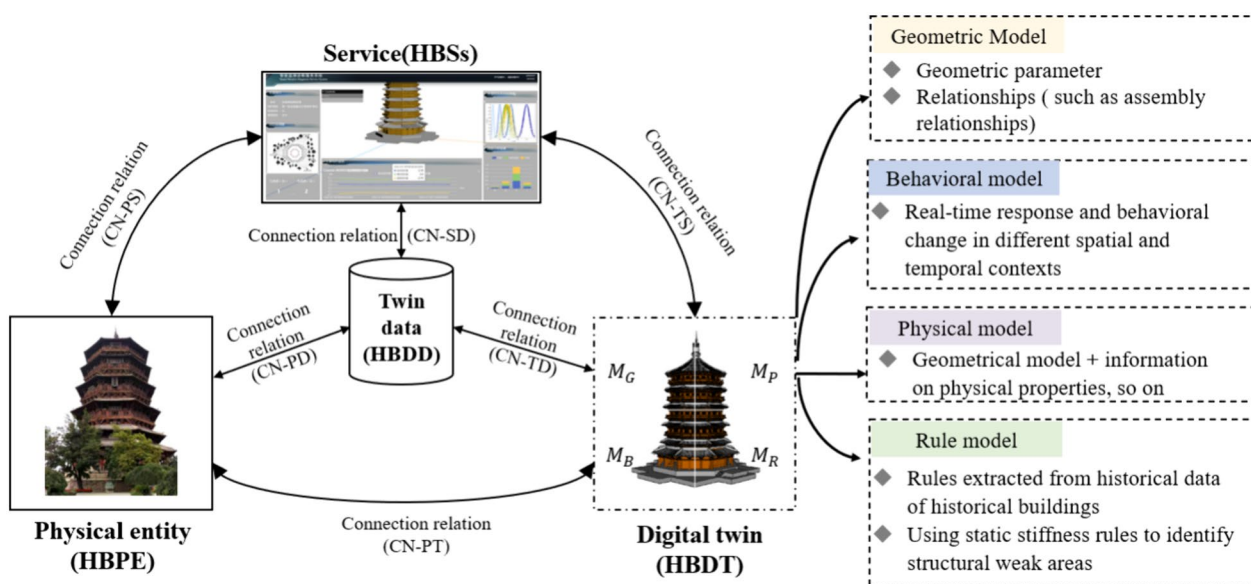


Fig. 2 Organizational chart of the digital twin of the historical building

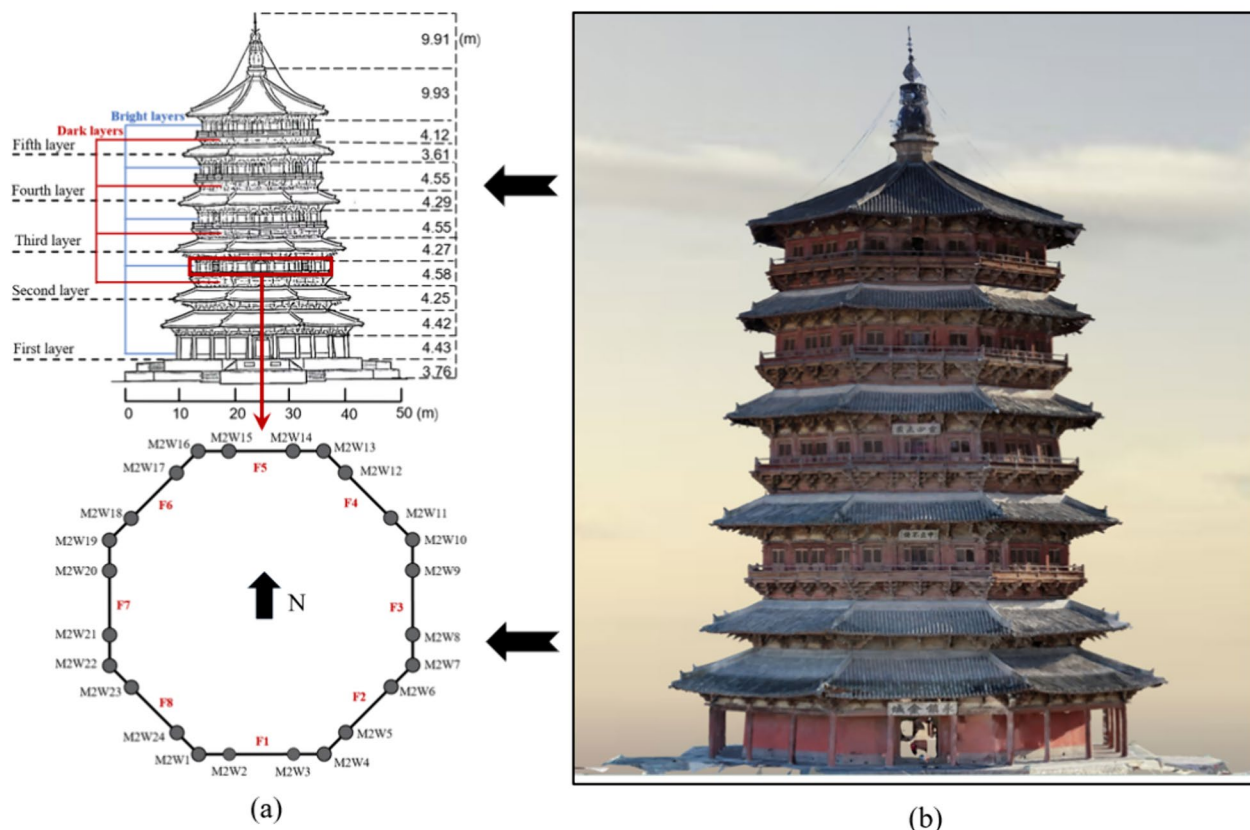


Fig. 3 Detailed size of the structure and front view of the structure

a more accurate registration. By setting up target control points, we aligned the internal and external point cloud data into an absolute coordinate system.

During the registration of the point cloud data, we use the Rodriguez matrix to calculate the parameters of the spatial transformations in order to construct a comprehensive point cloud model with absolute coordinates. The aligned point cloud model is pre-processed and then combined with multi-view images obtained from UAV tilt-photography, a combination that enhances the geometric accuracy of the model both locally and as a whole. This process pays special attention to the data integrity of high and occluded areas to ensure the comprehensiveness of the scanned data. In the end, our point cloud model was aligned to an accuracy of approximately 5.8 mm, which provided a solid data base for subsequent modelling and analysis work. The flowchart related to the registration can be found in Fig. 4.

Model data fusion program

The second layer of the hybrid model is built based on the high precision point cloud data obtained in sub-Sect. "On-site 3D scanning and registration program", and the model is intended to represent the real state of

the wooden pagoda in order to achieve the best accuracy in the prediction of the structural performance. Triangular mesh model, as a kind of discrete mesh model, has a strong descriptive ability for geometries with complex topology. Representing the individual surfaces of the model with triangular mesh not only gives a better visual effect, but also allows us to obtain 3D mesh models under different demands by controlling the number of triangular slices in the model. However, when fusing the triangular mesh model with the parametric model in some cases dealing with the wooden pagoda model, it may not be possible to connect the edges smoothly in some localized areas. This can result in complex polygonal holes that cannot be closed. These types of holes result in an overall model containing inaccurate geometry that cannot be imported into software such as Finite Element for analysis, and require area splitting as well as hole repair.

Hole repair in a triangular mesh model is in essence a problem of triangular sectioning of a spatial polygon. In order to ensure a smooth transition between the hole part and the mesh model, a repair algorithm is used to locally repair the polygonal holes that cannot be closed. First, the holes in the component mesh are identified by labeling the complex polygonal holes and performing a

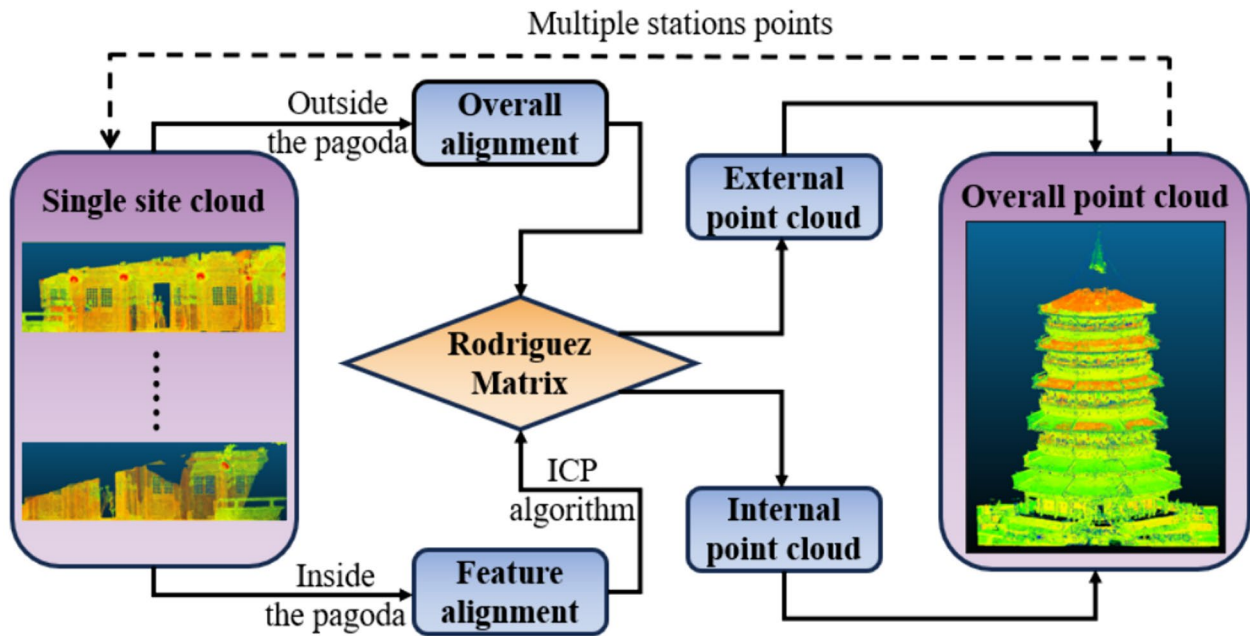


Fig. 4 Alignment flow chart

segmentation operation on these empty regions. Next, the repair process begins by determining the direction of hole shrinkage, a step that is performed by analyzing the normal vector pinch angle. Subsequently, the exact distance of the contraction is determined based on the distance relationship between the boundary edge of the hole and its neighboring edges. After completing the initial shrinkage, the boundary edges are optimized to ensure the formation of a closed boundary ring. Thereafter, new triangle segments are added based on a specific method, by iterating until the established termination conditions are satisfied. The process is shown in Fig. 5.

This process for hole repair in a structure involves five steps: First, identify the curvature mutation vertex and extend towards the hole boundary, finding feature folds based on the maximum angle. Second, segment the hole region to extract and shrink the boundary. Third, redefine the shrinkage direction and distance for boundary edges. Fourth, calculate the contraction distance. Fifth, determine the angle size of adjacent boundaries when constructing triangular slices, and iteratively recalibrate the boundary, shrinkage parameters, and add new triangles until the distance between boundary edges meets the contraction criteria. The process concludes with constructing a new triangular slice to finalize the hole repair.

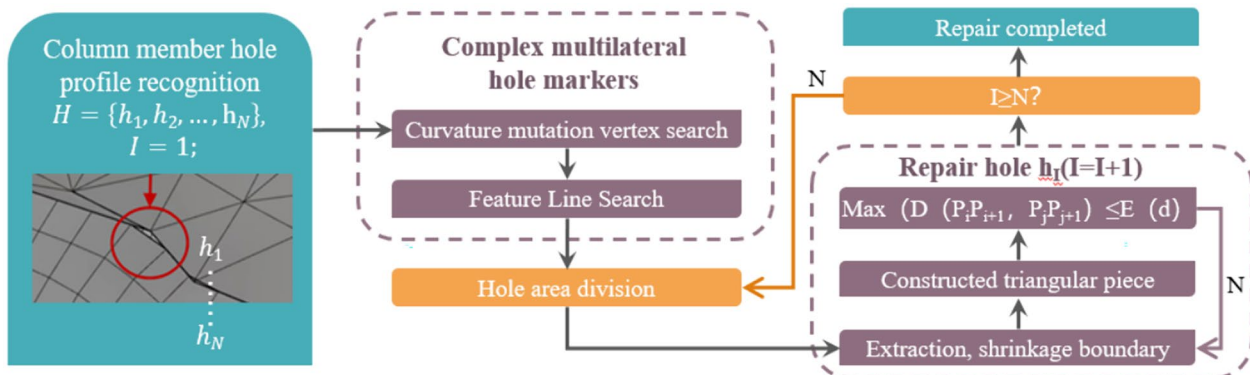


Fig. 5 Flow chart for repairing complex multilateral holes

To enhance the realism of surface shapes in models, non-uniform rational B-splines (NURBS) are employed for surface transformation, improving both geometric continuity and accuracy. This process converts original closed triangular meshes into multi-surface solids, more accurately simulating the aging damage of real column components and achieving seamless integration of null shortcoming clouds and real point clouds. The conversion involves preprocessing the mesh for simplification and repair, feature extraction for identifying geometric boundaries, and mesh parameterization by assigning parameters (u, v) to vertices. The transformation is primarily achieved through NURBS surface fitting:

$$S(u, v) = \frac{\sum_{i=0}^n \sum_{j=0}^m N_{i,p(u)} M_{j,q(v)} w_{ij} P_{ij}}{\sum_{i=0}^n \sum_{j=0}^m N_{i,p(u)} M_{j,q(v)} w_{ij}} \tag{1}$$

where P_{ij} is the control point, w_{ij} is the weight of the control point, $N_{i,p(u)}$ and $M_{j,q(v)}$ are B-spline basis functions. Ultimately, control points and weights were adjusted to optimize the surfaces, ensure proper continuity between adjacent surfaces, and further improve model quality through error detection and refinement. The final closed triangular mesh was converted to a closed multi-surface solid figure as shown in Fig. 6 below.

Taking the second layer of the wooden pagoda as the main study object, the second layer of the outer fluted column-architrave structure has a total of eight corner columns, namely, M2W1-S column, M2W4-S column, M2W7-S column, M2W10-S column, M2W13-S column, M2W16-S column, M2W19-S column, and M2W22-S column. Multi-phase point cloud comparisons were performed on eight corner posts to determine the orientation angle of the mortise and tenon interface at the endpoints to better reproduce the shape of the real wooden columns. Although this study has demonstrated a comprehensive approach through the use of UAV photogrammetry and LIDAR scanning to document in detail the process of data collection through to the creation of a hybrid model, there are several key issues that need to

be attended to in the mapping of complex historic buildings: limitations in equipment performance, occlusion issues, complexity of data processing, impact of material and surface properties, technical limitations, and constraints on laws and permissions. Addressing these issues requires the integration of technological innovations and methodologies to ensure data accuracy and completeness.

Digital twin geometry modeling

The construction of the geometric model meticulously depicts the shape, dimensions, structural details, spatial positioning of the column-architrave and its relationship to the environment. For the construction of the geometric models, the fidelity and level of simplification of the models are particularly important. These models not only reproduce the exterior shape, but their structural integrity and data accuracy also constitute the support for activities such as architectural historical research, structural analysis, restoration design, and digital display. The digital twin geometric model construction has three key components: fine modeling, decoupling of digital models, and geometric transformation, where the data for the fine model construction is derived from subSect. "3D scanning and model data fusion programs". In column-architrave structures, a single collection element constitutes a building element unit, and multiple building element units constitute a structural unit. As shown in Fig. 7.

Using this hierarchical modeling approach not only helps to maintain a clear organizational structure of the model, but also facilitates subsequent modification and optimization of the model to ensure a high degree of applicability and analytical efficiency. The process of constructing the geometric model of the digital twin is shown in Fig. 8.

Decoupling of digital models

Digital model decoupling is to split the ancient architecture structural model on the basis of setting the

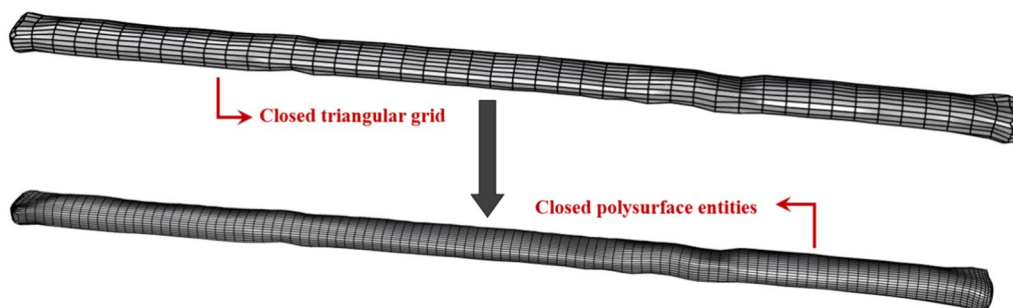


Fig. 6 Closed triangular mesh conversion to closed multi-surface solid maps

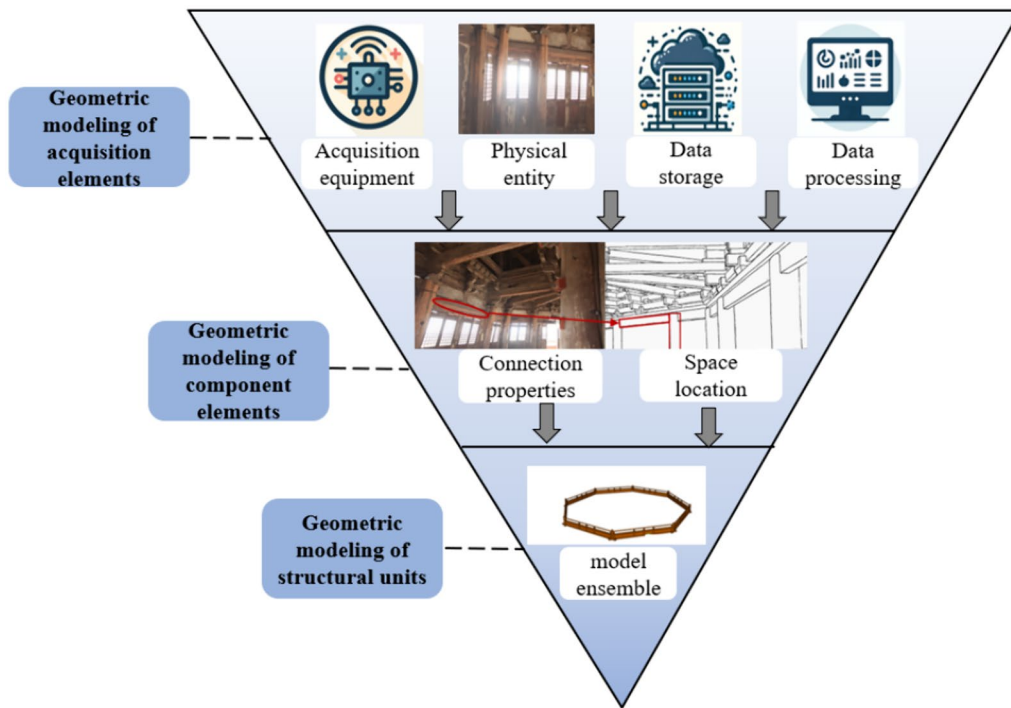


Fig. 7 Hierarchical modeling diagram

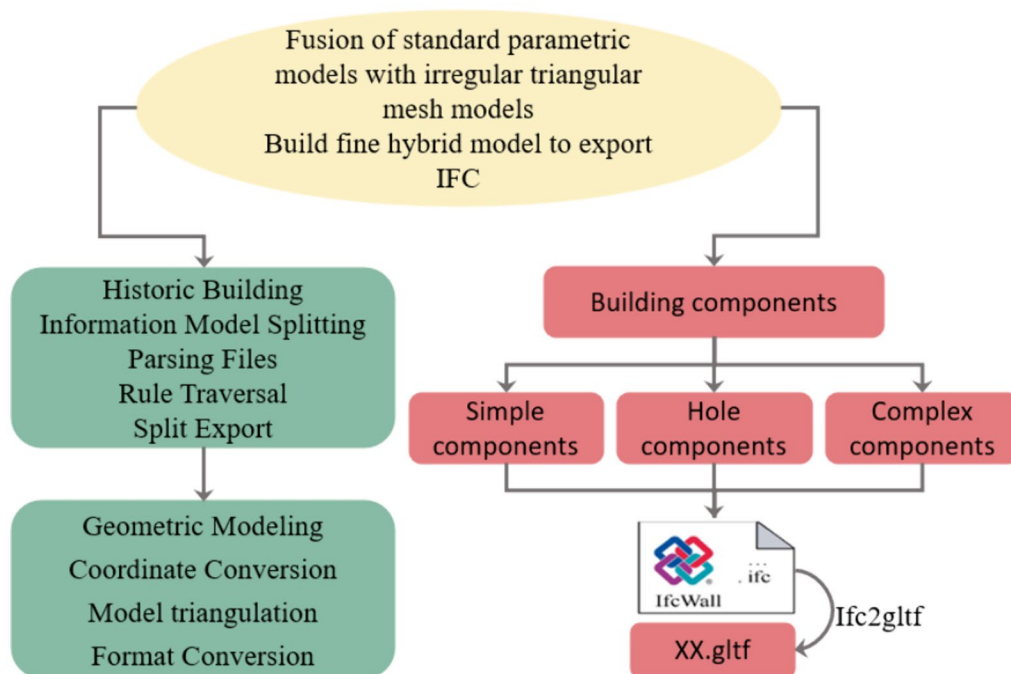


Fig. 8 Flowchart for the construction of the geometric model

ancient architecture information model splitting rules, forming subcomponents and realizing the accurate linking and preservation of its geometric and attribute information. Usually, the splitting rules of the ancient architecture information model are based on professional requirements and practical applications. In order to meet the subsequent digital twin management requirements, the IFC model is split mainly based on the classification of the ancient building component instances. By recursively accessing each node of the IFC structure tree, the geometric and property information of the ancient building component instances are hierarchically exported, laying the foundation for the subsequent digital twin visualization management model. The hierarchical IFC component export algorithm is shown in Table 1 below. According to the different geometrical characteristics of components, this study divides the splitting rules of the ancient building information model into the following three categories: (1) Simple component type. These types of components do not have holes or combined structures, such as columns and beams. They can be read directly by regular

query statements; (2) component types with holes. In IFC, holes are usually represented by “Opening” entities. In addition to the regular query, the hole field needs to be embedded and read through the association relationship; (3) Objects containing aggregated components. The Aggregates attribute in IFC can be used to identify the components that contain aggregated components. Based on the regular query, it is read based on the association attribute.

Geometric transformation

Geometry transformation is to efficiently render the geometric information of the model in the digital twin framework, and in this study, the glTF format is selected as the target for the transformation of the IFC model after the decoupling of the digital model. glTF (GL Transmission Format) is a file format designed for efficient network transmission and loading of 3D models, which uses key-value pairs to comprehensively describe the model's element combinations, materials, animations, and other information, covering all the content required for generating 3D scenes, and its internal structure is highly

Table 1 Hierarchical Export of Component Instances Based on IFC Structure Tree

Input: Historical building information modeling
Output: Example set of components with architectural relationships in a building model

```

Initialize queue Q for storing pending artifacts
Initialize collection A for storing geometry information
Initialize collection B for storing attribute information
for Each subcomponent of the building information model do
    if Components belong to predefined splitting rule definitions for construction types then
        Add component  $P_i$  to  $Q_i$ ;
    end if
end for
while Queue Q is not empty do
    for Geometric attribute information for each building element  $C_i$  in Q do
        if for geometric information then
            Add information to collection  $A_i$ ;
        else
            Adding property information to a collection  $B_i$ ;
        end if
    end for
end while
Returns the set of component instances

```

consistent with that of the WebGL rendering mechanism. A typical glTF model consists of a “.gltf” file, a “.bin” file and an img folder. The “.gltf” file is in JSON format and describes the structure and data configuration of the entire 3D scene. The “.bin” file stores the basic data of the model’s geometry in binary form, such as vertex information, normal vectors and texture coordinates. The “img” folder stores the texture resources needed by the model. glTF adopts detached design, usually only “.glTF” file is requested when loading, and external “.bin” file and texture resources are accessed through links to realize fast and efficient network transmission. glTF can be used for IFC model file conversion to accomplish the construction of geometric models in the digital twin framework. However, given the current technical limitations, it is difficult to convert directly from IFC format to glTF format. Therefore, this study chooses to use OBJ as an intermediate bridge to construct the IFC-OBJ-glTF conversion framework based on Java language, so as to realize the generation of glTF model files. Among them, the IFC-OBJ conversion mainly consists of three steps: ① analyzing and extracting the coordinates of the vertices of the triangular faces; ② analyzing and extracting the normal coordinates and texture values; ③ analyzing and extracting the material information.

Analysis of weak area identification of column-architrave structure based on static stiffness rule

Geometric model validation

The verification of the accuracy of the geometric model in this subsection is obtained by comparing the numerically simulated deformation of the geometric model with the deformation of the real column-architrave structure. Numerical simulation under certain conditions is performed on the established geometric model to obtain the deformation value, which is compared with the deformation of the real-time monitoring system. Certain conditions mainly refer to the finite element simulation and analysis of the geometric model without considering the temperature, humidity, wind speed and other conditions of the external environment, focusing on the impact of long-term self-weight loads. This approach was adopted in order to accurately assess the direct effect of deadweight on the stability of the structure in the early stages of the study. By focusing

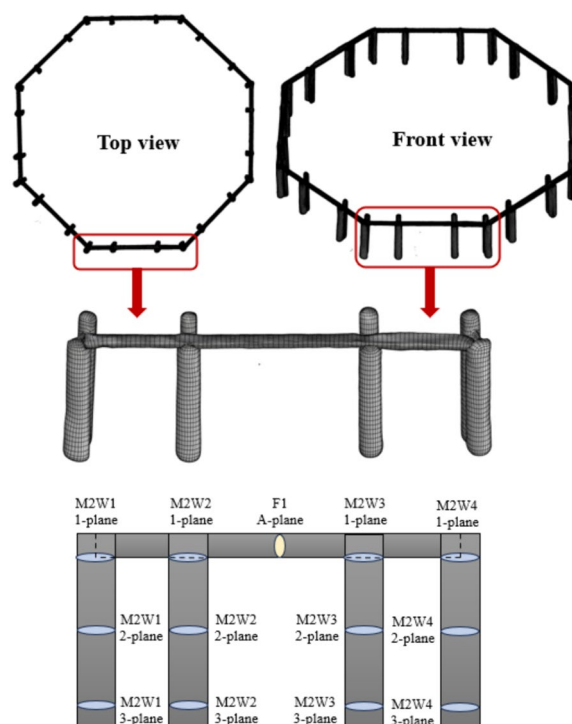


Fig. 9 Column-architrave structure analysis location schematic diagram

on the fundamental factor of long-term deadweight loading a solid foundation can be established for subsequent more complex analyses.

The material used for the column-architrave structure of the wooden pagoda is North China larch, which has orthogonal anisotropic properties. In the column-architrave structure, the main direction of force is longitudinal, bearing the vertical load transferred from the upper part. Material property parameters according to Table 2 [36].

The object for which the simulation analysis will be performed is the second layer of the structure consisting of 24 columns and 8 architraves. Example diagrams will be drawn on any one of the eight sides of the outside of the second layer, while the rest of the faces will have the same location of the stress points. Three analysis points are taken at the top, middle and foot positions of each column and are labeled as 1, 2, and 3. In addition, one analysis point is also taken at the middle position of each architrave and is

Table 2 Material parameters of wood

Material Density(Kg/m ³)	Elastic modulus (Mpa)			Poisson’s ratio		
	E _x	E _y	E _z	μ _{yz}	μ _{xz}	μ _{xy}
510.2	1000	275	650	0.3	0.02	0.035

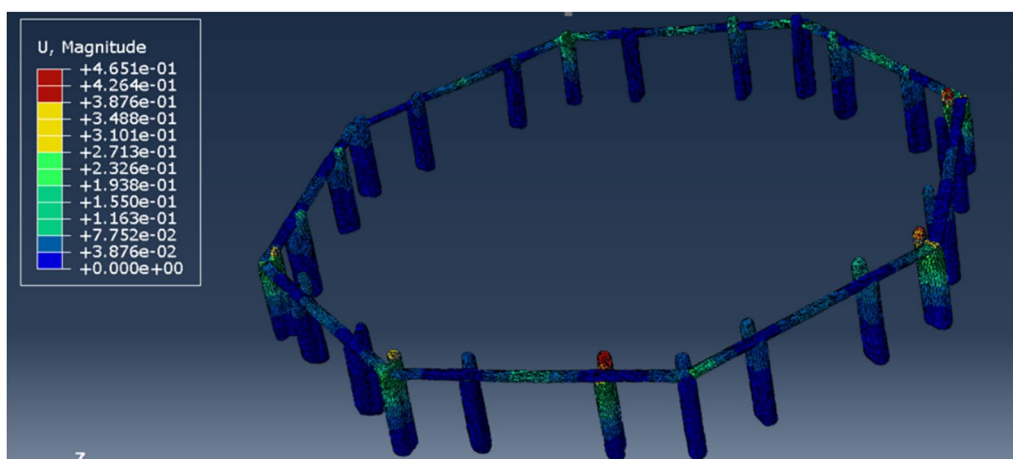


Fig. 10 Deformation cloud diagram of column-architrave structure

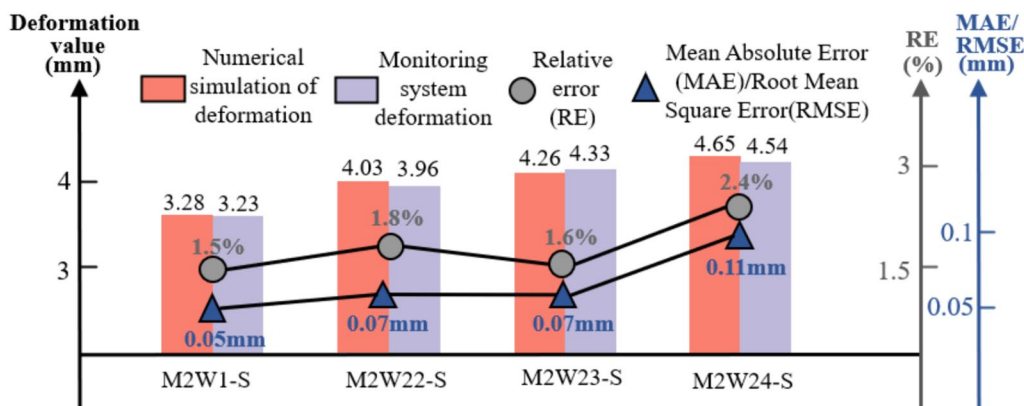


Fig. 11 Comparison of data from numerical simulation and real-time 3D monitoring system

labeled as A. The locations of the main stress points are shown in Fig. 9.

Our simulation is based on the original state of the wooden pagoda, taking into account all aspects of the performance of the wooden pagoda during its initial construction as well as the well-connectedness of the column and beam members. The mortise-and-tenon joints are considered as a whole in the simulation, and the column feet are in direct contact with the ground with fixed constraints at the feet. This simulation assumption reflects the actual condition of the wooden pagoda at the initial stage of construction in order to analyze the performance of the structure more accurately. In wooden pagoda structure, column members and architrave members mainly bear the vertical loads transmitted from the upper members such as the dougong and the pu-pai square. These loads are uniformly applied to the columns and architraves, including compressive and bending loads. Through the simulation, we obtained the deformation cloud as shown in Fig. 10,

according to which the behavior and performance of the structure is analyzed.

In order to verify the accuracy of the point cloud model, we selected four column locations in the simulated geometric model, namely, column M2W22-S, column M2W23-S, column M2W24-S, and column M2W1-S. Then, we compared and analyzed these positions with the data obtained from the real-time 3D monitoring system and recorded the error comparison results, in order to better assess the accuracy of the model, which are shown in Fig. 11.

The deformation data for numerical simulation are obtained by finite element simulation of a geometric model which is based on the actual collected point cloud data. The deformation data of the monitoring system, on the other hand, are derived from the real-time transmission of data from the buried sensors. Although there is a certain relative error in the numerical simulation, the relative errors between the numerical simulation results and the monitoring system are all within 3%. For the four column locations,

the deformation errors are all within 1 mm, which verifies the accuracy of the point cloud model.

Static stiffness rule analysis

Analysis of static stiffness rules for wooden columns

Combining the monitoring column deformation data every three months during the period 2021–2023 and the deformation simulation, a functional relationship between the deformation of the model and the static stiffness was established, that is, $E'_z I'_z = k E_z I_z$, with the help of this functional relationship and the deformations monitored in real time, the characteristic effect of the aging action on the static stiffness corresponding to time is known. Considering the wood column in the natural aging effect of the stiffness will be attenuated year by year, related research shows that the stiffness discount law is basically an exponential function form [29], the use of static stiffness discount coefficient to express the static stiffness of the wood column in this paper with the change rule of the service time, that is, get:

$$k = e^{at_z} \tag{2}$$

$$E'_z I'_z = k E_z I_z = e^{at_z} E_z I_z \tag{3}$$

Based on the form of the load-deformation function of the column under long-term deadweight loading, it was determined that the deformation of this wooden column was inversely proportional to the static stiffness (EI), that is:

$$\frac{y_z}{Y_z} = \frac{E'_z I'_z}{E_z I_z} = \frac{e^{at_z} E_z I_z}{E_z I_z} = e^{at_z} \tag{4}$$

where: k is the static stiffness reduction factor for wooden columns; t_z is the service time of the wooden column elements in years; a is a reduction constant; $E_z I_z$ represents the static stiffness of the wooden column in the initial state; $E'_z I'_z$ represents the static stiffness of a wooden column after taking into account the depreciating effects of natural aging; y_z represents the value of deformation of wooden columns under long-term loads; Y_z represents the value of deformation of wood columns under the combined effect of long-term loading + natural aging.

Multiple sets of numerical simulation data of the columns and real-time monitoring data were taken to calculate $a = -1.06 \times 10^{-3}$, $K = \frac{1}{e^{1.06 \times 10^{-3} \times t_z}}$. In this study, it is considered that the column is susceptible to instability when $K < 0.25$.

Analysis of static stiffness rules for wooden architraves

Similarly, the static stiffness reduction factor is introduced to represent the exponential function law of static

stiffness with service time of wooden architrave in this paper, which is obtained:

$$m = e^{bt_l} \tag{5}$$

$$E'_l I'_l = m E_l I_l = e^{bt_l} E_l I_l \tag{6}$$

$$\frac{y_l}{Y_l} = \frac{E'_l I'_l}{E_l I_l} = \frac{e^{bt_l} E_l I_l}{E_l I_l} = e^{bt_l} \tag{7}$$

where: m is the static stiffness reduction factor for wooden architraves; t_l is the service time of the wooden architrave elements in years; b is a reduction constant; $E_l I_l$ represents the static stiffness of the wooden architrave in the initial state; $E'_l I'_l$ represents the static stiffness of a wooden architrave after taking into account the depreciating effects of natural aging; y_l represents the value of deformation of wooden architraves under long-term loads; Y_l represents the value of deformation of wood architraves under the combined effect of long-term loading + natural aging.

Multiple sets of numerical simulation data of the architraves and real-time monitoring data were taken to calculate $b = -9.12 \times 10^{-4}$, $m = \frac{1}{e^{9.12 \times 10^{-4} \times t_l}}$. In this study, it is considered that the architrave is susceptible to instability when $m < 0.25$.

Analysis and identification of structural weak areas

First of all, it is necessary to determine the static stiffness of the structure in service so far, and the stiffness performance of the column-architrave structure is divided into column static stiffness performance and architrave static stiffness performance. Then, based on the known static stiffness rules in subSect. "Static stiffness rule analysis", the structure was evaluated and combined with 24 externally columns and 8 architraves, 10 critical points were selected at each of the top, middle and foot positions of the columns and the deformation values of each column at these three different positions were analyzed in depth, and finally, it was determined which areas might be weak or vulnerable.

According to subSect. "Static stiffness rule analysis", the static stiffness reduction factor of the column is calculated as $K = \frac{1}{e^{1.06 \times 10^{-3} \times t_z}} = \frac{1}{e^{1.06 \times 10^{-3} \times 968}} \approx 0.36$. At this time, the column is less prone to instability when $K > 0.25$. The static stiffness reduction factor of the architrave is calculated as $m = \frac{1}{e^{9.12 \times 10^{-4} \times t_l}} = \frac{1}{e^{9.12 \times 10^{-4} \times 968}} \approx 0.41$. At this time, the architrave is less prone to instability when $m > 0.25$. Based on the analysis of the instability condition of the column-architrave structure, the deformation values at several specific locations were analyzed to further

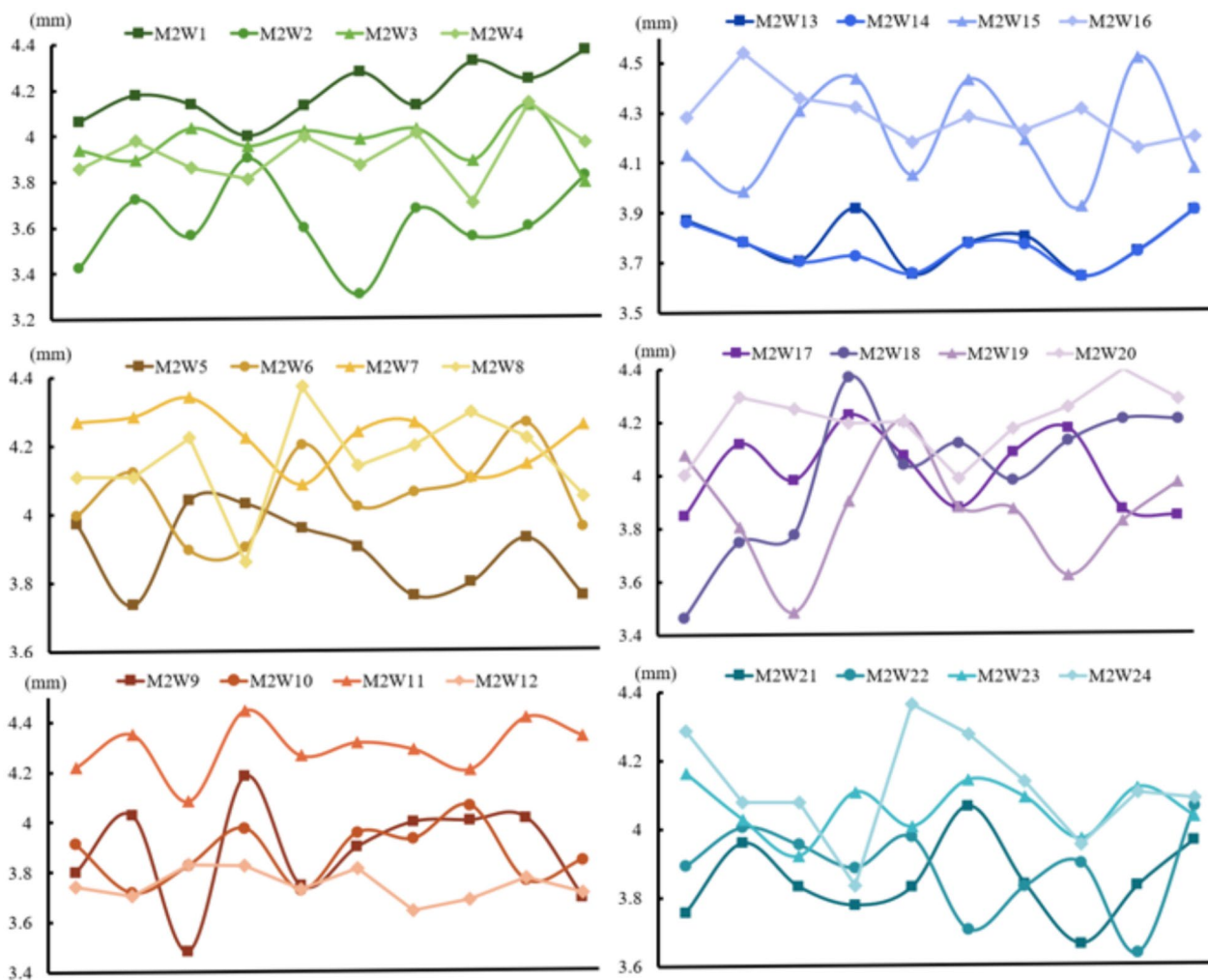


Fig. 12 Average deformation analysis of top, middle and foot of 24 columns

identify the potential weak areas of the structure, and the results were obtained as shown in Fig. 12.

The Yingxian wooden pagoda adopts an octagonal structure, and in the second layer of the column-architrave structure, we find that the deformation values of the four columns on the southwest side are significantly higher than those of the columns on the other sides. This implies that the columns on the southwest side may have been subjected to higher external forces or loads, thus leading to an increase in deformation. After analyzing the data of 24 columns in detail, we found that column M2W23 located on the southwest side of the wooden pagoda had the highest value of deformation at the top of the column, that is, at the height of one-third of the distance from the top to the bottom of the column, with a maximum value of 4.65 mm. According to the results of the calculations, the confidence interval for the average deformation value of column M2W23 at the 95%

confidence level is [4.472 mm, 4.828 mm]. Combined with the data in Fig. 11, it demonstrates that the column average is not excessive but the deformation at the top location is significantly large, and further structural analysis and reinforcement measures may be required to ensure its stability and safety. For the wooden pagoda structure, especially the columns on the southwest side, deformation analysis is critical. A comprehensive analysis of the data information of the 24 columns necessitated appropriate measures to address potential problems to ensure the health and safety of the structure.

Reinforcement assessment and optimization of architectural heritage digital twins

Reinforcement methods and material selection

Reinforcement methods and material selection for digital twins of ancient buildings, using digital twin technology,

are crucial for maintaining structural safety and preserving heritage. These methods should be tailored to the building's characteristics and condition, combining traditional techniques like wood or stone patching with modern materials like aluminum alloys or composites to enhance load-bearing and seismic capabilities without overburdening the structure. For instance, the entirely Yingxian wooden pagoda requires reinforcement that respects its original structure.

Generally, reinforcement for wooden structures is divided into two types: one is the strengthening reinforcement method, and the other is the damage repair reinforcement method. Considering the existing condition of the research object, we believe that the strengthening reinforcement method should be mainly considered. For the weak areas obtained in subSect. "Analysis and identification of structural weak areas", it is found that the wooden columns have been irreversibly deformed due to compression, and we adopt two kinds of reinforcement measures, traditional and modern, for the weak areas. The first traditional reinforcement method is mainly considered to be aluminum alloy reinforcement of the wooden columns, and the second modern reinforcement method is the use of Carbon Fiber Reinforced Polymer (CFRP) reinforcement.

Performance simulation and analysis of different reinforcement methods

Our study focuses on wooden pagoda external fluted columns, these members are subject to direct contact with the external environment and therefore face the challenge of material corrosion caused by external factors such as rainwater. When choosing a reinforcement

material, we need to consider the impact of the material's properties on the performance of the wooden columns. Given that aluminum alloys are similar to steel in many of their properties, and that aluminum alloys show better corrosion resistance and effective reinforcement of wooden columns, we chose aluminum alloys as the material for the first reinforcement solution. However, we also needed to be aware of the potential reduction in strength at high temperatures, the susceptibility of aluminum alloys to fatigue cracking, and their higher machining and welding costs. Considering the specific climatic conditions of the area where the wooden pagoda is located, high temperatures are not very frequent or extreme, so aluminum alloy became a suitable choice.

Option 1: The reinforcement method we used is double ring type reinforcement, this solution consists of two irregular rings of aluminum alloy material at the top and bottom and a long bar with a length of 95 cm. The main function of the long bar is to fix the two irregular rings. The wall thickness of the aluminum alloy tube is 7 mm and the height of both rings is 40 cm, which are mounted on one third and two thirds of the M2W23 wooden columns, respectively. Detailed construction dimensions are shown in Fig. 13.

Option 2: Through field investigations and extensive literature surveys, we have adopted an innovative reinforcement method using CFRP of different thicknesses for the existing wooden columns that are mostly damaged in appearance. The reinforcement solution, primarily achieved by bonding, is unique in that it offers several advantages. Firstly, the inherent lightness of the CFRP material helps to maintain the original structural stability of the wooden columns without introducing excessive

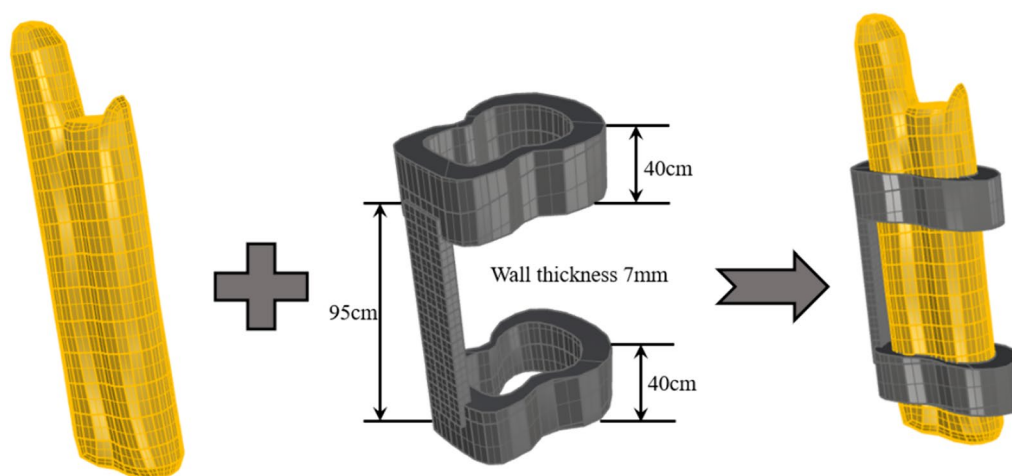


Fig. 13 Aluminum alloy reinforcement diagram

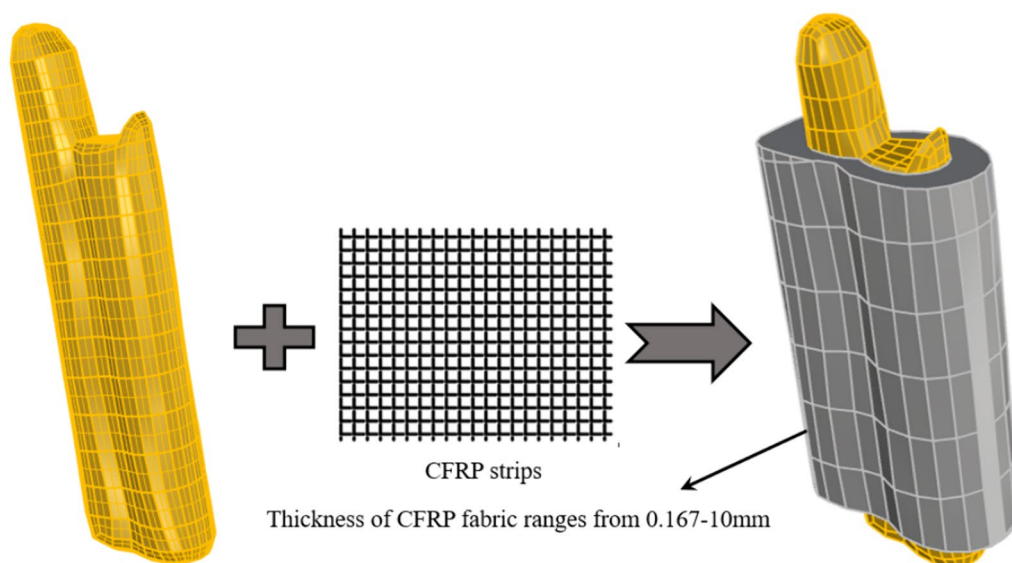


Fig. 14 Schematic diagram of CFRP reinforcement with different thicknesses

Table 3 Material parameters of aluminum alloy

Tensile strength /Mpa	Modulus of elasticity /Mpa	Poisson's ratio
273.1	70,698	0.32

Table 4 Material parameters of CFRP fabric

Tensile strength/Mpa	Modulus of elasticity/Gpa	Elongation/%
3483	231	1.7

additional loads, which is essential to maintain the structural integrity of the building. Secondly, CFRP fabrics can be cut as required, thus providing the flexibility to adapt to various shapes and sizes of wooden columns, regardless of the complexity of their geometric features, which makes the reinforcement process more precise and controllable. In addition, the excellent plasticity of the CFRP material allows it to adapt to the deformation of the wooden column, thus reducing the problems associated with mismatched stress distribution during the reinforcement process and ensuring that the reinforced wooden columns are better able to withstand external loads. Most importantly, this method of reinforcement is flexible enough to cope with uneven damage to wooden columns, with the CFRP fabric being able to reinforce the damaged areas as required to ensure an even distribution of strength throughout the column. The specific reinforcement is CFRP bonded around the entire column of the M2W23 wooden column, with a thickness range of

0.167–10 mm, depending on the condition of the salvage, as shown in Fig. 14.

The finite element simulations for both types of reinforcement follow the same parameter settings in Table 2. The parameters of the aluminum alloy material were configured according to the settings in Table 3, while the material parameters of the CFRP cloth were adjusted according to Table 4. For carbon fiber reinforced polymer, a linear elastic model was used for modelling. A contact gap of 0.001 mm was set in order to simulate the small gaps and non-linear contact behavior that are difficult to avoid in real situations. The adhesive slip between wood and CFRP cloth was not considered during the simulation. The boundary conditions are consistent with the experiments, the nodal displacements within the cross-section are constrained at both ends of the model and the degrees of freedom in the parallel grain direction are limited at one end, while the nodal displacements in the parallel grain direction are imposed at the other end and the nodal degrees of freedom are coupled.

Finite element simulations were carried out for the second layer of the external columns and we investigated two different reinforcement methods, that is, the use of aluminum alloy material and CFRP fabric. The results show that both aluminum alloy and CFRP fabric reinforcement significantly improved the structural stability of the wooden column M2W23. After aluminum alloy reinforcement, the deformation at the top of the wooden column was reduced to 3.5 mm, which is about 24.7% less compared to that before the reinforcement. The top deflection of the wooden column was reduced to 2.8 mm

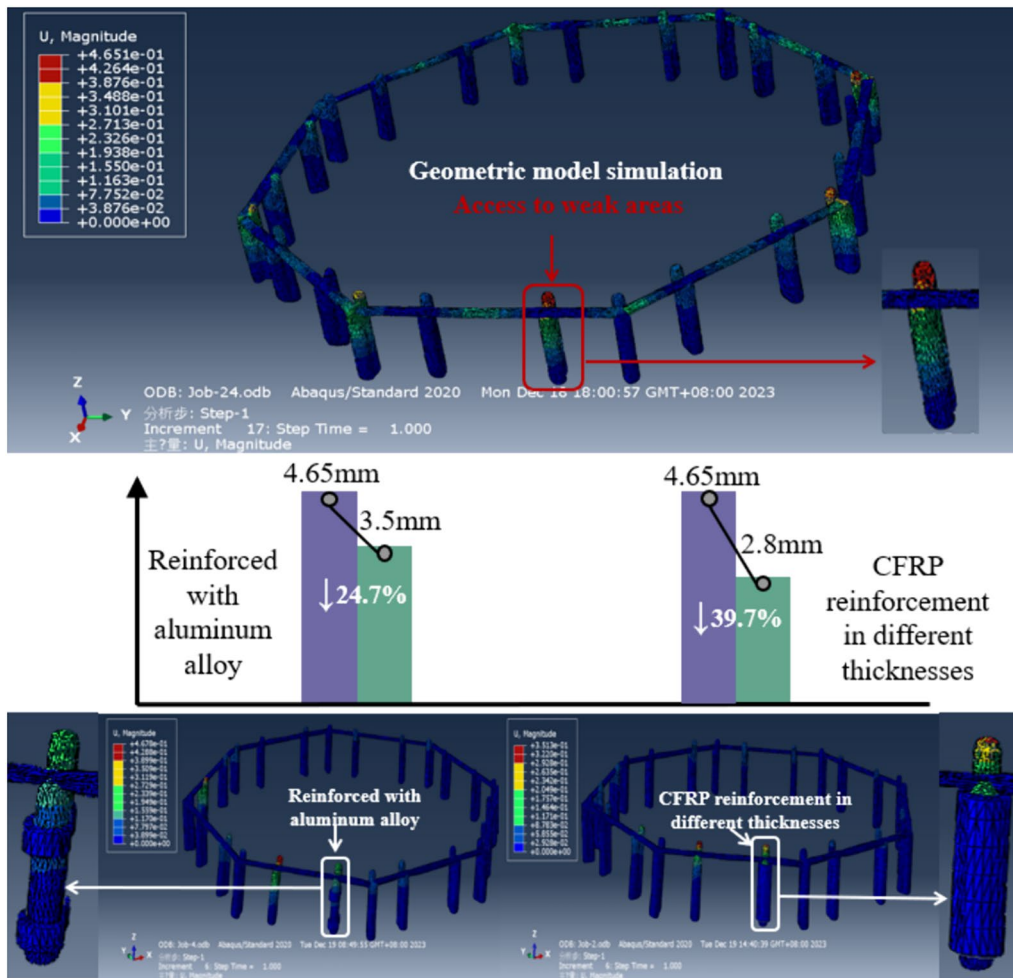


Fig. 15 Numerical simulation of two reinforcement options



Fig. 16 System presentation diagram for digital twins of ancient buildings

with CFRP fabric reinforcement, which is a reduction of about 39.7%. The paired t-test yielded a p-value ($1.8829e-06$) that is much smaller than the commonly used significance level (0.05). This indicates that the average difference between the two reinforcement methods is statistically significant, meaning that the impact of the reinforcement measures on deformation is significant and the difference is not due to random error. Although both methods were effective in reducing deformation, the CFRP reinforcement method was more suitable in this structure as it was more refined and was able to take into account the uniformity of the residual fabric. Taking into account factors such as regional precipitation, cost, performance requirements and feasibility, different thicknesses of CFRP reinforcement were required for this structure to improve the effectiveness of the reinforcement. As shown in Fig. 15.

Adjustment optimization strategies for digital twins

The adjustment and optimization strategy of digital twins plays an important role in the digital preservation of cultural heritage today. Through the digital twin technology, we are able to construct a systematic virtual model of the ancient buildings, which is a virtual model that can be used to map information such as real damages of real physical entities and interact with the actual ancient buildings in real time in order to monitor the state and behavior of the ancient buildings. The application of digital twin technology is crucial to the restoration of ancient buildings. Before carrying out the actual restoration, digital twin technology can provide accurate, intuitive and visualized prediction of the restoration effect to ensure that the restoration program is scientific and accurate, and avoid any defects that may cause irreversible damage to the ancient buildings. Based on this information, targeted optimization strategies can be developed and implemented to improve the efficiency, performance and reliability of the system. This intelligent means of adjustment and optimization not only reduces the cost and risk of ancient building restoration, but also promotes continuous improvement and innovation in cultural heritage protection. The final presentation of digital twin is shown in Fig. 16 below.

The specific digital twin adjustment and optimization strategies are as follows:

① Wooden pagoda real-time monitoring and feedback mechanism: the digital twin establishes a real-time feedback mechanism through real-time monitoring of the system's operating status, including a variety of sensor data and real-time monitoring information, as well as interaction with the actual system. This mechanism can discover abnormalities in the system operation in time, and quickly make responses and adjustments; ② Strategy

formulation based on scenario analysis: the digital twin evaluates the effects of different parameters, strategies or decisions on the system performance through virtual simulation experiments and analysis of different environments and scenarios of the system. Based on the effectiveness of the two reinforced methods verified, the digital twin system helps to simulate the operational status of the overall wooden pagoda structure after reinforcement; ③ Prediction and Risk Management: The digital twin identifies potential problems and risks in the system by analyzing and predicting historical and real-time data, so that preventive and management measures can be taken accordingly.

Conclusion and outlook

Main conclusions

This study employs LiDAR technology and multi-source point cloud data to construct a digital twin geometric model of the second layer of Yingxian wooden pagoda's column network, analyzing deformation and model accuracy. It identifies weak areas in the column-architrave structure by examining static stiffness and deformation at multiple points. Two reinforcement methods are tested on these areas, with their effects compared to determine the best reinforcement strategies and optimize future interventions.

- (1) Multi-period point cloud data were acquired using LiDAR technology, fusing the standard parametric model with the irregular triangular mesh model to more realistically reflect the existing shape of the column-architrave structure, and the digital twin geometric model was created through fine modeling→decoupling of digital models→geometric transformation, which provides a more refined structural stress analysis for the analysis model.
- (2) The constructed digital twin geometric model was accurately verified, and the stability assessment of the column-architrave structure was carried out based on the static stiffness rule, analyzing the deformation data at several points of the columns, and obtaining the weak areas—M2W23 column, whose deformations reached a maximum of 4.65 mm.
- (3) According to the characteristics of the Yingxian wooden pagoda and the condition of the existing structure, two different reinforcement methods were custom designed and their effects were comparatively analyzed. By comparing the reinforcement effects, it was found that the aluminum alloy material reduced the deformation of the wooden

columns from 4.65 mm to 3.5 mm, with a reduction of 24.7%. On the other hand, using CFRP reinforcement can further reduce the deformation to 2.8 mm, achieving a reduction of 39.7%. This indicates that CFRP is more effective in improving the structural strength of wooden columns.

- (4) Based on the digital twin system of the Yingxian wooden pagoda, the effect of the reinforcement method was verified, which helped to simulate the operational status of the overall wooden pagoda structure after reinforcement, and put forward a comprehensive adjustment and optimization strategy of real-time monitoring, scenario analysis, and risk management.

Future outlook

This study focuses mainly on the geometric dimension in the optimization methodology for reinforcement assessment of architectural heritage digital twins, while in-depth studies in other dimensions such as physical, behavioral and rule-based are still to be carried out. Considering the complexity of complete architectural heritage digital twins covering a wide range and in-depth details, future research needs to be further explored and developed. The present study, which mainly focuses on the second layer of the column-architrave structure, suggests that future research should examine more comprehensively all aspects of the wooden pagoda and the overall structural condition, and explore more reinforcement materials or techniques to assess their specific effects on different types of wooden structures.

Acknowledgements

This research was supported by the National Key Research and Development Program of China [Grant No. 2022YFF0904400]; National Natural Science Foundation of China [Grant No. 42171416, 41971350]; BUCEA Doctor Graduate Scientific Research Ability Improvement Project [Grant No. DG2024038].

Author contributions

Yanru Shi wrote the main manuscript text and prepared Figs. 1, 2, 3, 4, 5, 6, 7, 8, 9, 10, 11, 12, 13, 14, 15 and 16. Ming Guo is responsible for reviewing articles. Xuanshuo Liang is responsible for model building. Jiawei Zhao is responsible for data collation. Xiaoke Shang and Shuai Guo were responsible for literature research. Ming Huang is responsible for fund support. Youshan Zhao is responsible for data collation. The authors declare that this manuscript is original, has not been published before and is not currently being considered for publication elsewhere.

Funding

BUCEA Doctor Graduate Scientific Research Ability Improvement Project, DG2024038, National Key Research and Development Program of China, 2022YFF0904400, National Natural Science Foundation of China, 42171416, 41971350.

Data availability

No datasets were generated or analysed during the current study.

Competing interests

The authors declare that they have no known competing financial interests or personal relationships that could have appeared to influence the work reported in this paper.

Author details

¹School of Geomatics and Urban Spatial Informatics, Beijing University of Civil Engineering and Architecture, Beijing 102616, China. ²Engineering Research Center of Representative Building and Architectural Heritage Database Ministry of Education, Beijing University of Civil Engineering and Architecture, Beijing 100044, China. ³Beijing Key Laboratory for Architectural Heritage Fine Reconstruction & Health Monitoring, Beijing University of Civil Engineering and Architecture, Beijing 100044, China. ⁴National Construction Engineering Quality Supervision and Inspection Center, China Academy of Building Research, Beijing 100013, China.

Received: 14 March 2024 Accepted: 30 July 2024

Published online: 23 August 2024

References

- Grieves M. Virtually Intelligent Product Systems: Digital and Physical Twins. 2019. <https://doi.org/10.2514/5.9781624105654.0175.0200>
- Grieves M. Digital twin: manufacturing excellence through virtual factory replication. 2015.
- Tao F, Liu W, Zhang M, et al. Five-dimension digital twin model and its ten applications. *Comput Integr Manuf Syst*. 2019;25(1):1–18.
- Mandola C, Messeni Petruzzelli A, Percoco G, et al. Building a digital twin for additive manufacturing through the exploitation of blockchain: a case analysis of the aircraft industry. *Comput Ind*. 2019;109:134–52.
- SIEMENS. For a digital twin of the grid Siemens solution enables a single digital grid model of the Finnish power system.
- SWEDBERG C. Digital twins bring value to big RFID and IoT data.
- Dr. Hempel Digital Health Network. Healthcare solution testing for future. Digital Twins in healthcare.
- Gu J, Yang B, Dong Z, et al. Intelligent perfect-information surveying and mapping for digital twin cities. *Bull Survey Map*. 2020;06:134–40.
- Yu H, Yao D, Qian G, et al. Review of digital twin model of asphalt mixture performance based on mesostructure characteristics. *China J Highway Transport*. 2023;36(03):20–44.
- Lucchi E. Digital twins for the automation of the heritage construction sector. *Autom Constr*. 2023;156
- Vuoto A, Funari M, Lourenço P. Shaping digital twin concept for built cultural heritage conservation: a systematic literature review. *Int J Arch Herit*. 2023. <https://doi.org/10.1080/15583058.2023.2258084>.
- Li Y, Du Y, Yang M, et al. A review of the tools and techniques used in the digital preservation of architectural heritage within disaster cycles. *Herit Sci*. 2023. <https://doi.org/10.1186/s40494-023-01035-x>.
- Tan J, Leng J, Zeng X, et al. Digital twin for Xiegong's architectural archaeological research: a case study of Xuanluo Hall, Sichuan. *China Buildings*. 2022;12:1053.
- Guo M, Zhao J, Pan D, et al. Normal cloud model theory-based comprehensive fuzzy assessment of wooden pagoda safety. *J Cult Herit*. 2022;55:1–10.
- Guo M, Sun M, Pan D, et al. High-precision deformation analysis of Yingxian wooden pagoda based on UAV image and terrestrial LiDAR point cloud. *Herit Sci*. 2023;11(1):1–18.
- Cabaleiro M, Suñer C, Sousa H, et al. Combination of laser scanner and drilling resistance tests to measure geometry change for structural assessment of timber beams exposed to fire. *J Build Eng*. 2021;40: 102365.
- Cabaleiro M, Branco J, Sousa H, et al. First results on the combination of laser scanner and drilling resistance tests for the assessment of the geometrical condition of irregular cross-sections of timber beams. *Mater Struct*. 2018;51:99.
- Zhou J, Wang X, Qiao Y, et al. Techniques and methods of deformation monitoring of Yingxian wooden pagoda. *China Cult Herit*. 2021;101(01):39–44.

19. Guo M, Yan B, Zhou T, et al. Application of LiDAR technology in deformation analysis of Yingxian Wooden Pagoda. *J Archit Civ Eng*. 2020;37(02):109–17.
20. Guo M, Shi Y, Zhao Y, et al. Analysis of force deformation characteristics of aged wood column components with consideration of targeted hybrid fine modeling. *Int J Arch Herit*. 2023;17(11):1905–20.
21. Zhou T, Song X, Zhang L, et al. Experimental and numerical study on dou-gong joint of ancient wooden structure in qing dynasty. *Int J Arch Herit*. 2022. <https://doi.org/10.1080/15583058.2022.2113571>.
22. Xie Q, Zhang L, Xiang W, et al. Experimental study and finite element analysis of Dou Gong joints built with fork column under vertical loading. *J Build Struct*. 2018;39(09):66–74.
23. Xue J, Wu C, Hao F, et al. In situ experiment and finite element analysis on dynamic characteristics of Yingxian Wooden Tower. *J Build Struct*. 2022;43(02):85–93.
24. Xue J, Liang X, Song D, et al. Experimental study and finite element analysis on eccentric compressive performance of Dou-Gong brackets at column tops. *J Build Struct*. 2022;43(12):199–209.
25. He J, Wang J, Yang Q. Mechanical property of column footing joint in traditional wooden structure by quasi-static test. *J Build Struct*. 2017;38(08):141–9.
26. He J, Wang J, Yang Q. Theoretical and experimental analysis on mechanical behavior of column in traditional timber structure during rocking. *Eng Mech*. 2017;34(11):50–8.
27. Han X, Dai J, Qian W, et al. Effect of column foot tenon on behavior of larch column base joints based on concrete plinth. *BioResources*. 2020;15(3):6648–67.
28. Li S, Xie Q, Zhang B, et al. Compressive behavior of damaged timber columns: experimental tests, degradation model, and repair method. *Eng Struct*. 2023;293 <https://doi.org/10.1016/j.engstruct.2023.116579>.
29. Shi Y, Guo M, Zhou J, et al. Analysis of static stiffness properties of column-architrave structures of ancient buildings under long term load-natural aging coupling. *Structures*. 2024. <https://doi.org/10.1016/j.istruc.2023.105688>.
30. Xue J, Wu C, Zhang X, et al. Experimental study on seismic behavior of mortise-tenon joints reinforced with shape memory alloy. *Eng Struct*. 2020;218: 110839.
31. Xue J, Wu C, Zhang X, et al. Experimental and numerical study of mortise-tenon joints reinforced with innovative friction damper. *Eng Struct*. 2021;230: 111701.
32. Zhou L, Liu Q, Ma S, et al. Eccentric compression behavior of long poplar columns externally reinforced by BFRP. *J Wood Sci*. 2021;67(1):2.
33. İşleyen ÜK, Kesik H. Experimental and numerical analysis of compression and bending strength of old wood reinforced with CFRP strips. In *Structures*. 2021;33:259–71.
34. Pan Y, An R, You W, et al. A Mechanical Model Used for the Multifactor Analysis of Through-Tenon Joints in Traditional Chinese Timber Structures. *Int J Arch Herit*. 2023. <https://doi.org/10.1080/15583058.2023.2173106>.
35. Dong H, Jin Y, Cao W, et al. Seismic performance of wooden straight-tenon joints reinforced with lightweight steel members. *Eng Struct*. 2023;282: 115825.
36. Lu P. Analysis of the effect of aging on mechanical behavior of ancient timber structural members. Xi'an University of Architecture and Technology 2017.

Publisher's Note

Springer Nature remains neutral with regard to jurisdictional claims in published maps and institutional affiliations.